Effects of the nature and charge of the topmost layer in layer by layer self assembled amperometric enzyme electrodes

E. J. Calvo,*[a] V. Flexer,[b] M. Tagliazucchi[a] and P. Scodeller[a]

Received 5th May 2010, Accepted 26th July 2010
DOI: 10.1039/c0cp00449a

Organized layer-by-layer nanostructured amperometric enzyme electrodes with self-contained redox polyelectrolyte mediators have shown important effects depending on the nature and charge of the adsorbed topmost layer. Adsorption of PVS causes the drop of the catalytic responses to negligible values due to hindrance in electron hopping and enzyme wiring.

Introduction

Gero Decher introduced in 1991 organized multilayer films on solid substrates by alternate adsorption of anionic and cationic polyelectrolytes.[1–3] The strategy was extended to the adsorption of proteins[4] and to the development of amperometric enzyme electrodes based on layer-by-layer (LbL) self-assembled enzyme and redox mediator multilayers pioneered by Hodak *et al.*[5] in 1997. Since then an extensive literature has been published by our research group[6–12] and others[13–19] on amperometric enzyme electrodes comprised of LbL organized enzyme multilayers.

In these organized structures a much better control over the position of the redox polyelectrolyte with respect to the enzyme molecules than in random hydrogels built with the same components can be achieved; and spatially organized multilayers with mono and bi-enzymatic schemes can work efficiently in molecular recognition, redox mediation and generation of an electrical signal.[20]

Successive redox polymer mediator (either ferrocene or osmium complex tethered to polyallylamine backbone) and enzyme (Glucose Oxidase, GOx, Horseradish Peroxidase, HRP, Laccase, Lac, *etc.*) layers can be deposited by alternate immersion of the thiol-modified Au in the respective polyelectrolyte and enzyme solutions at suitable pH where the enzymes and polyelectrolytes exhibit the excess charge needed in the self-assembly process. The uptake of thiol, redox polymer, and enzyme on the surface can be monitored by quartz crystal microbalance and ellipsometry. Cyclic voltammetry shows surface waves of the redox centers in the polymer and the redox surface concentration can be obtained from integration of the low sweep rate voltammetric peaks in the absence of the enzyme substrate.

In layer by layer deposition it is expected that the enzyme film thickness, the surface concentration of redox sites and the enzyme loading all grow with the number of adsorption steps. Enzyme catalysis for different reactions such as the oxidation of glucose to glucono-lactone by glucose oxidase (GOx), the reduction of oxygen to water by laccase (Lac), was achieved with multilayers comprised of alternate enzyme and redox polymer layers.

The catalytic current varies with the film thickness and it has been established that the redox charge propagation within the film occurs by electron hopping with a diffusion coefficient that can be estimated from chrono-amperometric and impedance experiments. Thus, in these integrated supramolecular enzyme multilayer films a sequence of electron hopping events in the redox polymer is followed by electron transfer between some suitably positioned redox center and the enzyme prosthetic group.

While for thin films, only a small fraction of the active assembled GOx molecules are "electrically wired" by the redox polymer despite that all of the enzyme can be oxidized by soluble mediator,[5–8,20] it has recently been shown that the wiring efficiency increases with the number of layers and for films thicker than 300 nm the LbL enzyme multilayer approaches the behaviour of redox hydrogels.[21]

In their seminal work Hodak *et al.*[5] reported that the redox property of ferrocene modified poly(allyamine) multilayers depended significantly on the number of layers, with a decrease in redox charge for negatively charged GOx topmost layers. Furthermore, in the Faraday Discussion 2000 on Bioelectrochemistry it was shown that upon addition of a single layer of osmium complex derivatized polyallylamine, PAH-Os, adsorbed on top of the terminal GOx layer with the same enzyme concentration, the catalytic response was significantly larger and the amount of "wired enzyme" increased from 2.1 to 24% of the total enzyme present on the surface.[20]

Anzai demonstrated in 2003 that the redox properties of ferrocene containing polyelectrolyte multilayers (PEMs) depend on the deposition of outer layers even if these outer layers contain no redox sites:[22] The redox charge and the apparent redox potential changes depending on the nature of the topmost layer, either PAH or PVS with lower charge densities for PVS terminated layers and the effect was apparent both for thin and thick multilayer films. Xie and Granick[23] reported that the dissociation equilibrium of poly(metacrylic acid) in the inner PEMs significantly depends on the polarity of the strong polyelectrolyte deposited on the outermost surface of the film.

Unlike random polymers, LbL films exhibit the unique ability to control the nature and charge of the topmost layer

[a] *INQUIMAE. Fac. Ciencias Exactas y Naturales, Pabellon 2, Ciudad Universitaria, Argenina CP1428. E-mail: calvo@qi.fcen.uba.ar; Fax: 54114576 3341; Tel: 54114576 3378*
[b] *CRPP. Centre de Reserche Paul Pascal, 115 Av. Albert Schweitzer, 33600 Pressac, France*

at the polymer/solution interface. With polyanions and polycation constructs, not using enzymes, we have shown by electrochemical impedance spectroscopy (EIS) that polyanions terminated films exhibit a hindrance for redox switching as compared to polycation capped ones[12] but the nature of the slow process could not be unveiled with that technique. While the adsorption of the polyanion induces a decrease in the redox charge, increasing the ionic strength completely offsets the effect. In other words, the polyanion layer hinders the redox reversibility without physical loss of the redox centers. Trumpet analysis of cyclic voltammetry experiments and plots of normalized current *vs.* logarithm of sweep rate have shown that the adsorption of polyanions in the topmost layer affects the ability of the redox sites to exchange electrons, resulting in a decrease of the electron hopping diffusion coefficient by three orders of magnitude.[24]

In this paper we describe the unique ability of the layer-by-layer technique to systematically study the effects of adsorbing enzymes such as GOx and Lac and the polyelectrolytes PAH-Os and PVS in redox mediated enzyme multilayers.

Experimental

Reagents and materials

The following chemicals were used without further purification: sodium 3-mercapto-1-propanesulfonate (MPS), Aldrich glucose (Merck) and TRIZMA base and TRIS.HCl (Sigma). Doubly distilled water was purified with a Milli-Q reagent water system (Millipore®). Aqueous solutions of glucose oxidase (EC 1.1.3.4), from *Aspergillus niger* were prepared from Fluka reagent without further purification. Laccase from *Trametes trogii* was purified from stock cultures kept in malt extract agar slants at 4 °C.[25]

The complex $[Os(bpy)_2Cl(PyCOH)]Cl$ (PyCOH = pyridine-carbaldehyde) was prepared as previously reported, osmium poly(allylamine), (PAH-Os), was synthesized as described elsewhere.[26]

Gold coated Si(100) substrates were employed as electrodes with 20 nm Ti and a 20 nm Pd adhesion layer and a 200 nm gold layer thermally evaporated using an Edwards Auto 306 vacuum coating system, at $p < 1 \times 10^{-5}$ mbar. The quality of the Au surface was checked by cycling voltammetry (CV) in 2 M sulfuric acid between 0 and 1.6 V at 0.1 V s^{-1}.

Surface modification and characterization

Layer-by-layer supramolecular multilayers comprised of GOx or Lac and PAH-Os were prepared according to the process described by Hodak *et al.*[5] First, the gold surface was modified with sulfonate groups by immersion in a freshly prepared 20 mM 3-mercapto-1-propane sulfonic acid (MPS) solution for 30 min followed by rinsing with Milli-Q® water. After thiol adsorption, the first PAH-Os layer was formed by immersion of the thiol-modified Au substrate in a PAH-Os solution for 10 min. The next and subsequent layers were deposited onto the modified surface by alternate immersions in a 1 μM GOx or 8 μM Lac solution and 0.4 mM PAH-Os solution, respectively, for 10 min each, thoroughly rinsing in Milli-Q® water at the end of each adsorption step. The adsorption process was followed by *in situ* quartz crystal microbalance (QCM) and ellipsometry. A variable angle rotating-analyzer automatic ellipsometer (SE 400 model Sentech GmbH, Germany) equipped with a 632 nm laser as polarized light source was employed to measure the film thicknesses of the electrodes.

The quartz crystal resonator at 10 MHz was used as a quartz crystal microbalance (QCM) with a complex voltage divider to measure the resonant frequency and both components of the quartz crystal Butterworth–Van Dyke (BVD) equivalent circuit, which has been described elsewhere.[27] The crystals were mounted in the cells by means of viton O-ring seals, with only one face in contact with the electrolyte.

A standard three-electrode electrochemical cell was employed with an Autolab potentiostat (Eco-Chemie, Utrech, The Netherlands) with Ag/AgCl; 3M KCl reference electrode and a large-area platinum gauze counter electrode. All electrochemical experiments were carried out at room temperature.

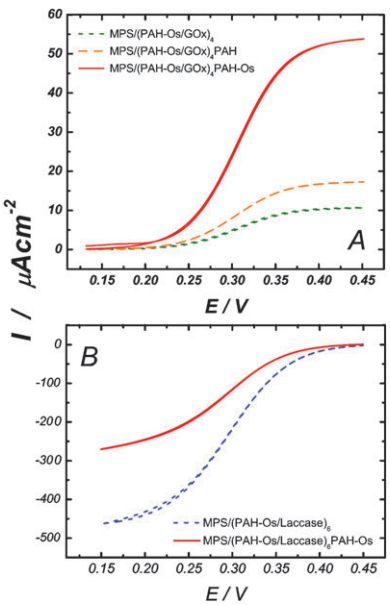

Fig. 1 Catalytic current-potential waves for GOx/PAH-Os (A) and Lac/PAH-Os (B) multilayers finished in negatively charged enzyme or in positively charged PAH-Os or PAH. Experiments were carried out in 20 mM TRIS buffer of pH 7.5, KNO_3 (I = 0.2 M), [glucose] = 50 mM for GOx/PAH-Os and 100 mM HAcO/NaAcO buffer of pH 4.7, KNO_3 (I = 0.2 M), pO_2 = 1 atm using a RDE (9 Hz) for Lac/PAH-Os. Scan rate: 5 mV s^{-1}.

Results and discussion

We describe the effects of adsorbing the topmost layer in enzyme multilayers comprised of the redox polycation PAH-Os and two anionic enzymes under similar adsorption conditions: GOx and Lac, respectively.

Fig. 1 depicts steady state redox-enzyme catalytic waves for the oxidation of glucose by GOx and mediated by PAH-Os(III)—Panel A—and the reduction of oxygen by Lac mediated by PAH-Os(II) -Panel B, respectively. In the first

case, a typical Nernstian dependence of the enzyme-redox catalytic wave in 50 mM glucose is observed as described elsewhere[9] for a negatively charged $(PAH\text{-}Os)_4(GOx)_4$ multilayer and a larger catalytic response for the same enzyme multilayer with further adsorption of a positively charged PAH-Os(+) topmost layer. However, addition of a polycation PAH(+) layer without the Os complex, also increases the catalytic current of a GOx terminated multilayer but to a lower level than for the PAH-Os(+) capped film. Therefore, two effects are operative:

(a) catalysis recovers by adsorption of PAH(+) or PAH-Os(+) onto a negative topmost layer which as shown by Anzai hinders the redox charge and;

(b) wiring from below and above the enzyme layer is more efficient than wiring only from below (as previously shown by Wolosiuk *et al.*)[28] and thus the catalysis is higher for the PAH-Os(+) capped film than for PAH (+) finished multilayer. For the system $(PAH\text{-}Os)_6(Lac)_6$, on the other hand, immersion in a solution of PAH-Os(+) produces a decrease in the catalytic current of the oxygen biocathode with respect to the Lac(−) topmost layer. In order to get an insight into this conflicting result we have studied the layer-by-layer deposition of PAH-Os(+) and both negatively charged redox enzymes by studying the evolution of the ellipsometric multilayer thickness and gravimetric mass by quartz crystal microbalance.

Fig. 2 depicts the steady state ellipsometric thickness and Fig. 3 shows the mass in each adsorption step: PAH-Os(+) and GOx(−) or Lac(−), respectively.

While for the GOx/PAH-Os system there is an increase of thickness and mass in every adsorption step, for the Lac/PAH-Os system after every adsorption from a PAH-Os(+) solution a decrease of mass and thickness of the multilayer is apparent. However, the total thickness and mass increases with the number of bilayer. Also, preliminary XPS experiments show a decrease in the Cu $2p_{3/2}$ signal after every PAH-Os(+) adsorption.[29]

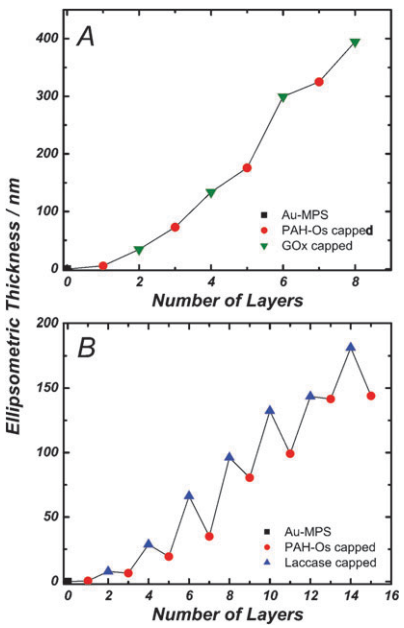

Fig. 2 Ellipsometric thickness for GOx/PAH-Os (A) and Lac/PAH-Os (B) multilayers as a function of the number of layers.

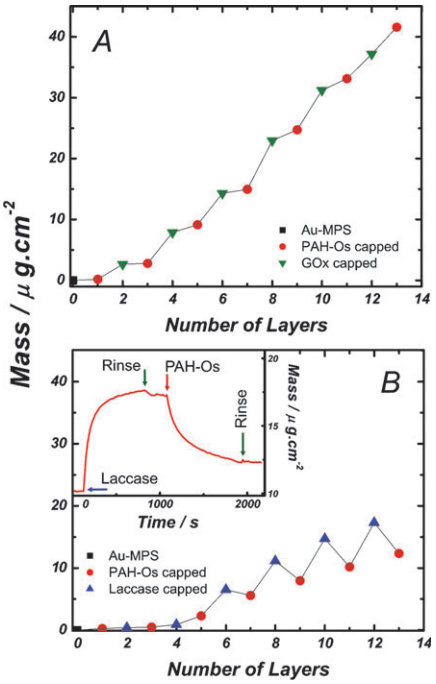

Fig. 3 Areal mass measured with QCM for GOx/PAH-Os (A) and Laccase/PAH-Os (B) multilayers as a function of the number of layers. Inset in B shows the mass transients for a $(PAH\text{-}Os/Lac)_5PAH\text{-}Os$ exposed to Lac solution in water, pure water rinsing, PAH-Os solution and finally water rinsing.

The inset in Fig. 3B depicts the time course of the adsorption of laccase, rinse and mass decrease upon adsorption of PAH-Os(+) on the Lac(−) terminal layer. These results are interpreted by partial desorption of laccase when exposed to solutions of highly charged polycation but the same is not observed for GOx(−) under similar conditions. It is suggested that laccase carries less negative charge on its surface than glucose oxidase under the conditions of the experiments which would explain its partial removal by the polycation.

The loss of enzyme would explain in the case of laccase why the catalytic current drops after adsorbing PAH-Os, while the nature and magnitude of charge in the outmost layer determines the behaviour of the GOx/PAH-Os system.

Hodak *et al.*[5] described a sawtooth effect of the observed redox charge in the absence of glucose for the GOx/ferrocene poly (allylamine) system, with a drop in redox charge after adsorption of the anionic enzyme. This drop in observed charge, which recovers after adsorbing the polycation, even if this does not contain the redox groups can be related to kinetic hindrance to address all redox sites in the experimental time window. Evidence of changes in the kinetics of charge transport has been obtained by electrochemical response in the absence of the substrate. The results of electrochemical impedance (EIS) for PAH-Os/GOx and PAH-Os/Lac films depicted in Fig. 4 show the electrode capacitance as a function of logarithm of the ac potential perturbation frequency ($\log_{10} f$). The capacitance was calculated as Y''/ω, where Y'' is the imaginary part of the impedance at the apparent redox

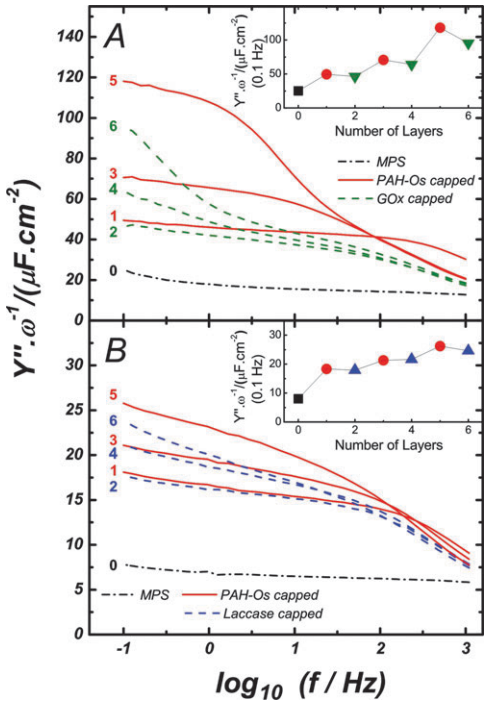

Fig. 4 (Y''/ω) *vs.* $\log_{10}$ (f) plots for PAH-Os$_m$/GOx$_n$ (A) and a PAH-Os$_m$/Lac$_n$ (B) films. The number at the left of each curve is the number of total adsorption steps, $(n+m)$. The insets show the low frequency (f = 0.1 Hz) capacitance as a function of the number of layers. Impedance spectra were acquired at $E = E^{0,\mathrm{app}}$ (see Fig. 6) in 20 mM TRIS buffer pH 7.5, I = 0.2 M (KNO_3) for PAH-Os/GOx and 0. 1M HAcO/NaAcO Buffer pH 4.7, I = 0.2 M (KNO_3) under Ar atmosphere for PAH-Os/Laccase.

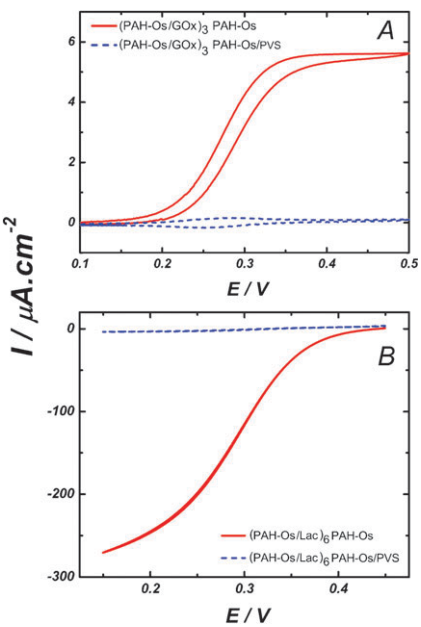

Fig. 5 Catalytic current-potential waves for PAH-Os/GOx (A) and PAH-Os/Lac (B) multilayers finished in positively charged PAH-Os or negatively charged PVS. Experiments were carried out in the same conditions of Fig. 1.

potential of the Os(III)/Os(II) (which varies due to the Donnan potential,[30] see Fig. 6) and $\omega = 2\pi f$. Curves for GOx/PAH-Os (Fig. 4A) and Laccase/PAH-Os (Fig. 4B) multilayers bearing a different number of layers are shown. For non redox mercaptopropane sulfonated modified Au electrode (Au/MPS) the only contribution to the capacitance arises from non-Faradaic processes (double layer charge) and thus the capacitance is frequency independent, $Y''/\omega = C_{DL}$ (where C_{DL} is the double layer capacitance).

Electrodes bearing at least one PAH-Os layer show an additional contribution to the electrode capacitance given by the oxidation/reduction of the osmium complexes, *i.e.* a redox capacitance. Thus the low frequency capacitance is proportional to the redox charge in the layer.[12]

The redox reaction within the film behaves as a diffusion process and therefore in an experiment with a characteristic time $\tau = 1/f$ only those sites located at a distance $(2.D_{\mathrm{app}}\cdot\tau)^{1/2}$ from the electrode can be electrochemically addressed. This implies that at very high frequencies (higher than those shown in Fig. 4), the only contribution to electrode capacitance is C_{DL} and therefore all curves should converge. At lower frequencies the diffusion wave penetrates deeper into the film resulting in an increase of the capacitance. Finally when the diffusion wave reaches the electrolyte/film interface, a constant capacitance is observed, *i.e.* $Y''/\omega \approx C_{DL} + C_{REDOX}$, where C_{REDOX} is that redox capacitance related to the number of osmium sites per unit area (Γ_{Os}) by:

$$C_{\mathrm{REDOX}} = \frac{F^2 A \Gamma_{\mathrm{Os}}}{4RT} \qquad (1)$$

The curve for 5 layers in Fig. 4A, $(\mathrm{PAH\text{-}Os/GOx})_2\mathrm{PAH\text{-}Os}$, follows this ideal description. From the frequency where the curvature of the curve changes ($f_{tr} \approx 0.3$ Hz, the frequency where the diffusion wave reaches the solution/film boundary) and the film thickness (d) we can estimate a diffusion coefficient of $D_{\mathrm{app}} = d^2 \cdot f_{tr}/2 = 2 \times 10^{-10}$ cm^2 s^{-1}, very similar to that observed for PAH-Os capped PAH-Os/PVS multilayers.[24,30,31] Comparison with the curves in Fig. 4A with 1 and 3 layers shows that the transition frequency is shifted to higher values when decreasing the film thickness, as expected from $f_{tr} = 2D_{\mathrm{app}}/d^2$. Unfortunately, the ideal behavior described above is not observed for the other spectra in the figure because C_{DL} and C_{REDOX} are not ideal capacitances.

An interesting feature observed in Fig. 4 is that the films capped with PAH-Os (odd number of layers) show systematically a higher capacitance than those with an additional enzyme layer. In particular, the insets in the figures show that the low frequency capacitance increases upon adding PAH-Os and decreases after enzyme adsorption. The effect has been previously reported for PAH-Os/polyanion films and ascribed to a decrease in the electron-hopping diffusion coefficient for polyanion capped films.[12] It is also worthwhile noting that the effect is less marked for enzymes than for synthetic linear polyanions such as PVS and more marked for GOx than for Lac. This result may indicate an important role of the charge density of the negatively charged macromolecule (it is suggested to increase in the order Lac < GOx < PVS), which can also be related to the

observation that the effect of the outmost layer can be offset by increasing the ionic strength.[12]

Since the effect of the outmost layer on the electrochemical response seems to be stronger for PAH-Os/PVS films than for PAH-Os/enzyme, we studied the effect of an additional PVS layer on the redox kinetics and electrocatalytic performance of PAH-Os/GOx and PAH-Os/Laccase multilayers.

Fig. 5 shows that dipping GOx and Lac multilayers terminated in PAH-Os(+) in solutions of the polyanion PVS(−) results in a sharp decrease of the steady state enzyme catalytic current. Thus, in both cases the negatively charged linear polyelectrolyte has a strong inhibition effect on either mediated enzyme catalytic reaction.

Fig. 6 shows the CV in absence of substrate before and after adding an extra PVS layer on top of a PAH-Os capped PAH-Os/enzyme films. A sharp drop in the redox charge (electrochemically addressable osmium sites) as well as an increase in peak separation are observed both for Lac and GOx multilayers. Fig. 6B shows that upon increasing the ionic strength from 0.2 to 2 M for the PVS capped film, there is an almost complete recovery of the redox charge. This is evidence that there is no desorption of the redox polymer PAH-Os during the adsorption of PVS as confirmed by the QCM.

This result is consistent with the almost complete absence of the catalytic activity for PVS capped electrodes in Fig. 5.

A quantitative analysis of the effect shown in Fig. 6 can be done by determining the electron hopping diffusion coefficient with different capping polyelectrolytes. Recently, variable scan rate cyclic voltammetry has been successfully used for this purpose for PAH-Os/PVS films.[24]

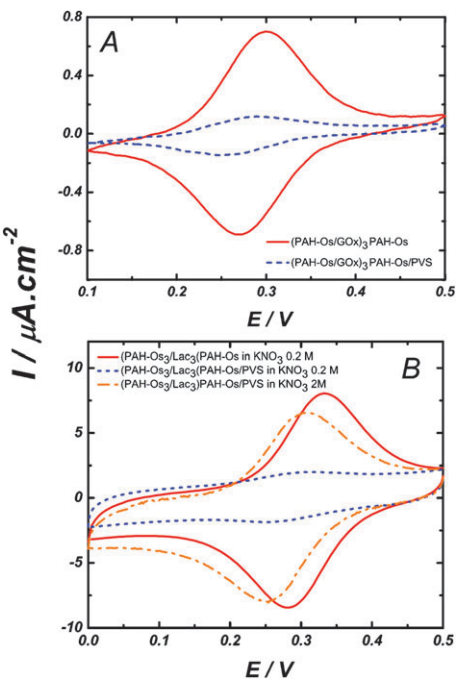

Fig. 6 Cyclic voltammetry for PAH-Os/GOx (A) and PAH-Os/Lac (B) multilayers finished in positively charged PAH-Os or negatively charged PVS. Experiments were carried out in the same conditions of Fig. 4, using $v = 5$ mV s^{-1} for PAH-Os/GOx and $v = 100$ mV s^{-1} for PAH-Os/Lac.

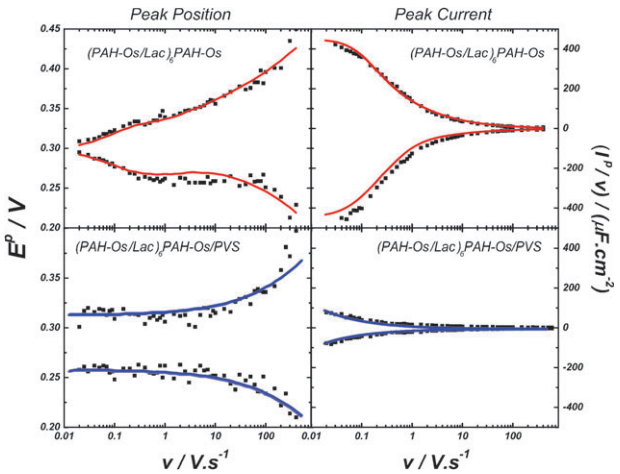

Fig. 7 Scan rate dependence of the peak potential position (left panels) and the peak current normalized by the scan rate (right panels) for the oxidation and reduction waves of Lac/PAH-Os multilayers finished in PAH-Os (upper panels) and PVS (lower panels). Measurements were performed in 0.1 M HAcO/NaAcO buffer pH 4.7, $I = 0.2$ M (KNO_3) under Ar. Solid lines show the best fit with the diffusion model previously described.[24]

Fig. 7 depicts the scan rate dependence of the experimental anodic and cathodic peak potential position and peak currents (divided by the scan rate) for PAH-Os and PVS capped PAH-Os/Lac multilayers. The peak separation for the positively capped film is almost zero in the low scan rate limit indicating complete redox switching under thin layer conditions.

However, increasing the scan rate produces an increase in the peak separation; from the Laviron model it is expected for a diffusion-limiting process *ca.* 58 mV.[32,33] On the other hand, the PVS finished film exhibits this peak separation even for the lowest scan rate, indicating that thin layer behavior cannot be achieved in the scan rate range under analysis. For $v > 50$ V s^{-1} a linear dependence of the oxidation and reduction peak potentials with log(v) for both films suggest a limitation in charge transfer at the electrode/film interface. Peak currents for the PVS capped film are much smaller than for a film with PAH-Os in the top layer showing the hindrance of the redox process in the former.

The experimental data was fitted to a diffusion model described elsewhere[24] assuming that the film thickness and the total number of redox sites remain constant during PVS adsorption. Best fit values for PAH-Os capped film were D_{app}: 1×10^{-10} cm^2 s^{-1}, k_0: 2.4×10^{-4} cm s^{-1}, $E^{0,app}$: 0.297 V, δ_A: 10 nm and $\Delta E_A^{0,app}$: 0.020 V (see ref. 24 for definitions of δ_A and $\Delta E_A^{0,app}$). Best fit values for PVS capped film were D_{app}: 1×10^{-12} cm^2 s^{-1}, k_0: 5×10^{-5} cm s^{-1}, $E^{0,app}$: 0.285 V, δ_A: 0 nm and $\Delta E_A^{0,app}$: 0.0 V.

The dramatic 100-fold drop in the apparent electron hopping diffusion coefficient, D_{app}, from 1×10^{-10} to 1×10^{-12} cm^2 s^{-1} upon PVS adsorption is similar to that previously determined for the non enzymatic PAH-Os/PVS films during the adsorption of PVS.[24]

Fig. 8 shows the time evolution of the catalytic current (panel A), the low frequency capacitance (panel B) and the change of the imaginary (ΔX_L) and real part (ΔR) of the

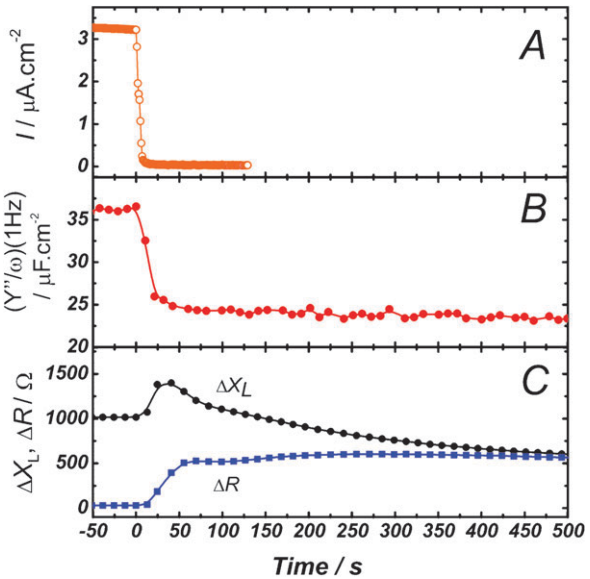

Fig. 8 Time evolution of the electrode capacitance measured at 1 Hz and $E = E^{0,app}$ (A), electrocatalytic current at $E = 0.5$ V and [glucose] = 50 mM (B), and QCM response (C) for the adsorption of PVS on a $(PAH\text{-}Os/GOx)_3PAH\text{-}Os$ film (A, B) or $(PAH\text{-}Os/GOx)_6PAH\text{-}Os$ (C). The experiments were performed in 20 mM TRIS buffer pH 7.5, $I = 0.2$ M. (KNO_3). At $t = 0$ a concentrated PVS solution was added to yield a final 20 mM PVS concentration.

quartz crystal impedance with reference to the bare crystal in water, upon PVS adsorption.[34] The transient in Fig. 8A shows a sharp decay to almost zero catalytic current upon PVS adsorption, in agreement with the CV experiment in Fig. 5A. The low frequency capacitance in Fig. 8B also decreases during PVS adsorption. As discussed above, this quantity accounts for the double layer capacitive component (independent of film thickness) and a redox component related to the number of electrochemically addressable osmium sites that increases with the number of adsorbed redox layers. Thus PVS assembly causes a decrease in the redox charge that can be accessed in the experimental timescale even though there is no loss of osmium into the solution. Note that the PVS induced decay in the transient of Fig. 8A is faster than that observed in Fig. 8B and that the catalytic current becomes negligible even when the cyclic voltammetry of PVS capped film in Fig. 6B still shows an Os(II)/Os(III) redox peak. This suggests that PVS may hinder not only the site to site electron hopping across the film, but also the ability of the osmium complex to wire the enzyme. The QCM transients in Fig. 8C show that both ΔR and ΔX_L ($\omega\Delta L$) components of the BVD electrical equivalent circuit of the lumped element[34,35] quartz crystal/Au/enzyme multilayer are affected by PVS adsorption due to significant viscoelastic changes during adsorption of the polyanion.[36] The QCM transients show a fast process where both ΔX_L and ΔR rapidly increase with a characteristic time of $\sim$10 s, followed by a slower process that can be related to slow film molecular reorganization.

It is suggested that the same process induced by the PVS adsorption that attenuates the acoustic wave in the enzyme films (increase in ΔR) is responsible for the 100-fold decrease of the electron hopping between redox sites that results in reduction of addressable redox charge and drop in the catalytic current.

Conclusions

The catalytic current in amperometric enzyme electrodes built layer-by-layer by self-assembly of negatively charged enzymes and redox active polycations, depends on the nature of the topmost layer.

For GOx(−) containing multilayers capped in the osmium polycation there is a higher catalytic rate than for films finished in the electroinactive cation, and these show higher activity than a film capped with negatively charged GOx(−).

For laccase, adsorption of the polycation removes partly the topmost enzyme layer resulting in a decrease of the catalytic current.

The role of charge has been elucidated by adsorbing the highly charged linear PVS(−) on the redox polycationic topmost layer and it is to hinder the electron hopping mechanism and the wiring of the enzyme by the redox polyelectrolyte. Viscoelastic changes detected with the QCM are consistent with changes in the enzyme multilayer structure during the adsorption of negative PVS.

References

1 G. Decher, *Science*, 1997, **277**, 1232–1237.
2 G. Decher, J. D. Hong and J. Schmitt, *Thin Solid Films*, 1992, **210–211**, 831–835.
3 G. Decher and J. D. Hong, *Ber. Bunsen-Ges. Phys. Chem.*, 1991, **95**, 1430–1434.
4 Y. Lvov, K. Ariga, I. Ichinose and T. Kunitake, *J. Am. Chem. Soc.*, 1995, **117**, 6117–6123.
5 J. Hodak, R. Etchenique, E. J. Calvo, K. Singhal and P. N. Bartlett, *Langmuir*, 1997, **13**, 2708–2716.
6 E. J. Calvo, C. Danilowicz and A. Wolosiuk, *J. Am. Chem. Soc.*, 2002, **124**, 2452–2453.
7 E. J. Calvo, C. B. Danilowicz and A. Wolosiuk, *Phys. Chem. Chem. Phys.*, 2005, **7**, 1800–1806.
8 E. J. Calvo, R. Etchenique, L. Pietrasanta, A. Wolosiuk and C. Danilowicz, *Anal. Chem.*, 2001, **73**, 1161–1168.
9 V. Flexer, E. S. Forzani and E. J. Calvo, *Anal. Chem.*, 2006, **78**, 399–407.
10 P. Scodeller, V. Flexer, R. Szamocki, E. J. Calvo, N. Tognalli, H. Troiani and A. Fainstein, *J. Am. Chem. Soc.*, 2008, **130**, 12690–12697.
11 R. Szamocki, V. Flexer, L. Levin, F. Forchiasin and E. J. Calvo, *Electrochim. Acta*, 2009, **54**, 1970–1977.
12 M. E. Tagliazucchi and E. J. Calvo, *J. Electroanal. Chem.*, 2007, **599**, 249–259.
13 S. X. Zhang, W. W. Yang, Y. M. Niu, Y. C. Li, M. Zhang and C. Q. Sun, *Anal. Bioanal. Chem.*, 2006, **384**, 736–741.
14 A. Narvaez, G. Suarez, I. C. Popescu, I. Katakis and E. Dominguez, *Biosens. Bioelectron.*, 2000, **15**, 43–52.
15 N. Anicet, C. Bourdillon, J. Moiroux and J. M. Saveant, *J. Phys. Chem. B*, 1998, **102**, 9844–9849.
16 K. Sirkar, A. Revzin and M. V. Pishko, *Anal. Chem.*, 2000, **72**, 2930–2936.
17 X. Q. Cui, R. J. Pei, X. Z. Wang, F. Yang, Y. Ma, S. J. Dong and X. R. Yang, *Biosens. Bioelectron.*, 2003, **18**, 59–67.
18 N. Anicet, A. Anne, J. Moiroux and J. M. Saveant, *J. Am. Chem. Soc.*, 1998, **120**, 7115–7116.
19 H. C. Yoon and H. S. Kim, *Anal. Chem.*, 2000, **72**, 922–926.
20 E. J. Calvo, F. Battaglini, C. Danilowicz, A. Wolosiuk and M. Otero, *Faraday Discuss.*, 2000, **116**, 47–65.
21 V. Flexer, E. J. Calvo and P. N. Bartlett, *J. Electroanal. Chem.*, 2010, **646**, 24–32.

22 A. H. Liu and J. Anzai, *Langmuir*, 2003, **19**, 4043–4046.
23 A. F. Xie and S. Granick, *J. Am. Chem. Soc.*, 2001, **123**, 3175–3176.
24 M. Tagliazucchi and E. J. Calvo, *ChemPhysChem*, 2010, DOI: 10.1002/cphc.201000172.
25 P. Scodeller, R. Carballo, R. Szamocki, L. Levin, F. Forchiassin and E. J. Calvo, *J. Am. Chem. Soc.*, 2010, DOI: 10.1021/ja1020487.
26 C. Danilowicz, E. Corton and F. Battaglini, *J. Electroanal. Chem.*, 1998, **445**, 89–94.
27 E. J. Calvo, C. Danilowicz and R. Etchenique, *J. Chem. Soc., Faraday Trans.*, 1995, **91**, 4083–4091.
28 E. J. Calvo and A. Wolosiuk, *ChemPhysChem*, 2005, **6**, 43–47.
29 E. J. Calvo, F. Williams, M. Tagliazucchi and P. Scodeller, in preparation.
30 M. Tagliazucchi, F. J. Williams and E. J. Calvo, *J. Phys. Chem. B*, 2007, **111**, 8105–8113.
31 M. Tagliazucchi, D. Grumelli, C. Bonazzola and E. J. Calvo, *J. Nanosci. Nanotechnol.*, 2006, **6**, 1731–1740.
32 E. Laviron, *J. Electroanal. Chem. Interfacial Electrochem.*, 1980, **112**, 1–9.
33 E. Laviron, L. Roullier and C. Degrand, *J. Electroanal. Chem. Interfacial Electrochem.*, 1980, **112**, 11–23.
34 S. J. Martin, H. L. Bandey, R. W. Cernosek, A. R. Hillman and M. J. Brown, *Anal. Chem.*, 2000, **72**, 141–149.
35 R. W. Cernosek, S. J. Martin, A. R. Hillman and H. L. Bandey, *IEEE Trans. Ultrason. Ferroelectr. Freq. Control*, 1998, **45**, 1399–1407.
36 E. J. Calvo, E. Forzani and M. Otero, *J. Electroanal. Chem.*, 2002, **538–539**, 231–241.